

## Numerical Treatment of Casson Fluid Free Convective Flow Past An Infinite Vertical Plate Filled in Magnetic Field in Presence Of Thermal Radiation: A Finite Element Technique

**R. Srinivasa Raju**

Department of Mathematics, GITAM University, Hyderabad Campus, Rudraram, 502329, Telangana State, India  
Email address: [srivass999@gmail.com](mailto:srivass999@gmail.com)

Received date: December 2016

Accepted date: December 2016

### Abstract

The combined effects of hall current, thermal radiation on an unsteady MHD free convection casson fluid flow of a viscous, incompressible and electrically conducting fluid past an infinite vertical plate are investigated in presence of heat transfer. Numerical solutions of the non-linear coupled governing equations is obtained by finite element technique. The expressions for primary fluid velocity, secondary fluid velocity and fluid temperature, skin friction due to primary and secondary velocity fields and rate of heat transfer coefficient due to temperature at the plate are obtained and discussed with the help of different material parameters like Grashof number for heat transfer, Casson fluid parameter, Magnetic field parameter, hall parameter, thermal radiation parameter, Prandtl number. Finally, it is seen that the numerical results of the present study conform very well to those of previous studies reported in available scientific literatures.

**Keywords:** Hall current, Casson fluid, MHD, Thermal Radiation, Finite element method

### 1. Introduction

The description of the laws of physics for space and time-dependent problems are usually expressed in terms of partial differential equations (PDEs). For the vast majority of geometries and problems, these PDEs cannot be solved with analytical methods. Instead, an approximation of the equations can be constructed, typically based upon different types of discretizations. These discretization methods approximate the PDEs with numerical model equations, which can be solved using numerical methods. The solution to the numerical model equations are, in turn, an approximation of the real solution to the PDEs. The finite element method (FEM) is used to compute such approximations. The finite element method is a numerical method for solving problems of engineering and mathematical physics. The words "finite element method" were first used by Clough in his paper in the Proceedings of 2<sup>nd</sup> ASCE (American Society of Civil Engineering) conference on Electronic Computation in 1960. Several authors are applying finite element method in their research problems. Baltacioğlu et al. [1] studied large deflection analysis of laminated composite plates resting on nonlinear elastic foundations by the method of discrete singular convolution. Shu et al. [2] studied the applications of generalized differential and integral quadrature to solve boundary layer equations. Civalek et al. [3] studied discrete singular convolution approach for buckling analysis of rectangular Kirchhoff plates subjected to compressive loads on two-opposite edges. The combined effects of heat and mass transfer on unsteady MHD natural convective flow past an infinite vertical plate enclosed by porous medium in the presence of thermal radiation and Hall Current was

investigated by Ramana Murthy et al. [4]. Rao et al. [5] found the numerical results of the non-linear partial differential equations of free convective magnetohydrodynamic flow past semi-infinite moving vertical plate with the effects of thermal radiation and viscous dissipation using finite element technique. Srinivasa Raju [6] studied the combined effects of thermal-diffusion and diffusion-thermo on unsteady free convection fluid flow past an infinite vertical porous plate in the presence of magnetic field and chemical reaction using the finite element technique. Srinivasa Raju [7] studied the combined effects of Soret and Dufour on natural convective fluid flow past a vertical plate embedded in porous medium in presence of thermal radiation via finite element method. Srinivasa Raju et al. [8] studied the joint influence of transpiration and hall effects on unsteady magnetohydrodynamic free convection fluid flow over an infinite vertical plate using finite element method. Srinivasa Raju et al. [9] studied unsteady magnetohydrodynamic free convective flow past a vertical porous plate with variable suction by applying finite element technique. Sailaja et al. [10] found the numerical solutions of double diffusive effects on magnetohydrodynamic mixed convection casson fluid flow towards a vertically inclined plate filled in porous medium in presence of biot number using finite element technique.

The study of non-Newtonian fluids is an important topic for researchers due its industrial applications in construction of paper production, polymer sheet, hot rolling, glass-fabric, wire drawing and petroleum production. The tangent hyperbolic fluid, Maxwell fluid, Williamson fluid, viscoelastic fluids, etc. are non-Newtonian fluids describing the nonlinearity behaviour. Casson fluid model is one of the most commonly used rheological model and has number of examples such as blood, fruit juices, soup, sauce, chocolate, etc. A magnetohydrodynamics (MHD) flow of non-Newtonian fluid was first studied by Sarpkaya [11] and then followed by many authors. The two-dimensional flow over unsteady stretching surface presented by Mukhopadhyay et al. [12]. Mukhopadhyay et al. [13] found numerical solutions for a steady heat transfer in a Casson fluid boundary layer flow over exponentially stretching permeable surface in presence of heat flux. Raju et al. [14] discussed Casson fluid over an exponentially porous stretching sheet in presence of heat and mass transfer effects. Das et al. [15] analyzed the combined effects of heat and mass transfer for unsteady Casson fluid in a vertical plate. Mahanta et al. [16] studied the concepts of magnetohydrodynamic 3D Casson fluid flow pass a porous linear stretching sheet. The influence of thermal radiation on unsteady free convection flow of an electrically conducting, gray gas near equilibrium in the optically thin limit along an infinite vertical porous plate were investigated by Seddeek and Aboeldahab [17] in the presence of strong transverse magnetic field imposed perpendicularly to the plate, taking hall currents into account.

The main goal of this paper is to find the numerical solutions using a powerful technique namely the finite element method for the primary and secondary velocities and temperature distributions to study the unsteady magnetohydrodynamics casson fluid flow over a vertical plate in the presence of hall current and thermal radiation. The effects of different involved parameters such as grashof number for heat transfer, magnetic field parameter, hall parameter, thermal radiation parameter, angle of inclination, Prandtl number on the primary and secondary fluid velocities and temperature distributions are plotted and discussed.

## 2. Mathematical formulation

The simultaneous effects of thermal radiation and hall current on unsteady MHD free convective Casson fluid flow over a vertical plate in presence of heat transfer is studied. For this present investigation, let  $x'$ -axis is taken to be along the plate and  $y'$ -axis normal to the plate. Since the plate is considered infinite in  $x'$ -direction, hence all physical quantities will be independent of

$x'$ –direction. Therefore, all the physical variables become functions of  $y'$  and  $t$  only. The wall is maintained at constant temperature  $T'_w$  higher than the ambient temperature  $T'_\infty$  respectively. All the fluid properties except the density in the buoyancy force term are constant and the plate is electrically non-conducting. The viscous dissipation and the joule heating effects are negligible in the energy equation. A uniform magnetic field of magnitude  $B_o$  is applied normal to the plate. The transverse applied magnetic field and magnetic Reynolds number are assumed to be very small, so that the induced magnetic field is negligible. Also, assumed that the electric field is neglected. The rheological equation of state for the Cauchy stress tensor of Casson fluid [18] is written as

$$\tau = \tau_0 + \mu\alpha^* \quad (1)$$

$$\text{equivalently } \tau_{ij} = \begin{cases} 2\left(\mu_B + \frac{p_y}{\sqrt{2\pi}}\right)e_{ij}, & \pi > \pi_c \\ 2\left(\mu_B + \frac{p_y}{\sqrt{2\pi_c}}\right)e_{ij}, & \pi < \pi_c \end{cases} \quad (2)$$

where  $\tau$  is shear stress,  $\tau_0$  is Casson yield stress,  $\mu$  is dynamic viscosity,  $\alpha^*$  is shear rate,  $\pi = e_{ij}e_{ij}$  and  $e_{ij}$  is the  $(i, j)^{th}$  component of deformation rate,  $\pi$  is the product based on the non-Newtonian fluid,  $\pi_c$  is a critical value of this product,  $\mu_B$  is plastic dynamic viscosity of the non-Newtonian fluid,

$$p_y = \frac{\mu_B \sqrt{2\pi}}{\gamma} \quad (3)$$

denote the yield stress of fluid. Some fluids require a gradually increasing shear stress to maintain a constant strain rate and are called Rheopectic, in the case of Casson fluid (Non-Newtonian) flow where  $\pi > \pi_c$ .

$$\mu = \mu_B + \frac{p_y}{\sqrt{2\pi}} \quad (4)$$

Substituting Eq. (3) into Eq. (4), then, the kinematic viscosity can be written as

$$\nu = \frac{\mu}{\rho} = \frac{\mu_B}{\rho} \left(1 + \frac{1}{\gamma}\right) \quad (5)$$

However, Cogley et al. [19] showed that, in the optically thin, limit for a gray gas near equilibrium the following relation holds:

$$\frac{\partial q_r}{\partial y} = 4(T' - T'_w)I \quad (6)$$

$$\text{Where } I = \int_0^\infty K_{\lambda w} \left( \frac{\partial e_{b\lambda}}{\partial T} \right)_w d\lambda$$

With all the above assumptions and the usual boundary layer and Boussinesq's approximation are ([17]):

*Equation of Continuity:*

$$\frac{\partial v'}{\partial y'} = 0 \quad (7)$$

*Momentum Equations:*

$$\frac{\partial u'}{\partial t} + v' \frac{\partial u'}{\partial y'} = \nu \left( 1 + \frac{1}{\gamma} \right) \frac{\partial^2 u'}{\partial y'^2} - \frac{\mu_e^2 \sigma B_0^2}{\rho(1+m^2)} (u' + mw') + g\beta(T' - T'_\infty) \quad (8)$$

$$\frac{\partial w'}{\partial t} + v' \frac{\partial w'}{\partial y'} = \nu \frac{\partial^2 w'}{\partial y'^2} + \frac{\sigma B_0^2 \mu_e^2}{\rho(1+m^2)} (mu' - w') \quad (9)$$

*Energy equation:*

$$\frac{\partial T'}{\partial t} + v' \frac{\partial T'}{\partial y'} = \frac{\kappa}{\rho C_p} \frac{\partial^2 T'}{\partial y'^2} - \frac{4(T' - T'_w)}{\rho C_p} I \quad (10)$$

The corresponding boundary conditions are given by

$$\left\{ \begin{array}{l} t' \leq 0: \{u' = 0, \quad w' = 0, \quad T' = 0 \quad \text{for all } y'\} \\ t' > 0: \left\{ \begin{array}{l} u' = 0, \quad w' = 0, \quad T' = T'_w \quad \text{at } y' = 0 \\ u' \rightarrow 0, \quad w' \rightarrow 0, \quad T' \rightarrow T'_\infty \quad \text{at } y' \rightarrow 0 \end{array} \right. \end{array} \right\} \quad (11)$$

We now define the similarity variables as follows:

$$u' = u_0 u(y), \quad w' = u_0 w(y), \quad \theta(y) = \frac{(T' - T'_\infty)}{(T'_w - T'_\infty)}, \quad y = \frac{y'}{h} \quad (12)$$

Where  $h (= h(t))$  is a similarity parameter length scale and  $u_0$  is the free stream velocity. In terms of  $h(t)$ , a convenient solution of (7) can be given by  $v' = -v_0 \left( \frac{u}{h} \right)$  (13)

Where  $v_0$  is a non-dimensional transpiration parameter, clearly  $v_0 > 0$  and  $v_0 < 0$  indicates suction or injection respectively. Substituting (12) and (13) in Eqs. (8), (9) and (10) yields

$$-\frac{h}{\nu} \frac{\partial h}{\partial t} yu' - v_0 u' = \left( 1 + \frac{1}{\gamma} \right) u'' - (Gr)\theta + \frac{M}{(1+m^2)} (u + mw) \quad (14)$$

$$-\frac{h}{\nu} \frac{\partial h}{\partial t} yw' - v_0 w' = w'' + \frac{M}{(1+m^2)} (mu - w) \quad (15)$$

$$-\frac{h}{\nu} \frac{\partial h}{\partial t} y \theta' - \nu_o \theta' = \frac{1}{\text{Pr}} \theta'' - R(\theta - 1) \quad (16)$$

Where  $Gr = g\beta h^2 \frac{(T'_w - T'_\infty)}{\nu u_o}$ ,  $\text{Pr} = \frac{\rho \nu C_p}{k}$ ,  $M = \frac{\sigma \mu_e^2 B_o^2 h^2}{\nu \rho}$ ,  $R = \frac{4Ih^2}{\rho C_p \nu}$

The boundary conditions corresponding to the Eqs. (14), (15) and (16) are

$$\left. \begin{aligned} u = 0, \quad w = 0, \quad \theta = 1 \quad \text{at } y = 0 \\ u \rightarrow 0, \quad w \rightarrow 0, \quad \theta \rightarrow 0 \quad \text{as } y \rightarrow \infty \end{aligned} \right\} \quad (17)$$

Eqs. (14), (15) and (16) are similar except for the term  $\left(\frac{h}{\nu}\right)\left(\frac{\partial h}{\partial t}\right)$  where  $t$  appears explicitly. Thus, the similar condition requires that  $\left(\frac{h}{\nu}\right)\left(\frac{\partial h}{\partial t}\right)$  must be constant.

Hence it is assumed that  $\left(\frac{h}{\nu}\right)\left(\frac{\partial h}{\partial t}\right) = C_1$  (18)

Where  $C_1$  is an arbitrary constant. At  $C_1 = 2$  and by integrating equation (18), one obtain  $h = 2\sqrt{vt}$  which defines the well-established scaling parameter for unsteady boundary layer problems ([20]). Hence, the similarity equations are obtained as

$$\left(1 + \frac{1}{\gamma}\right) u'' + 2(y + a_o) u' = -(Gr)\theta + \frac{M}{(1+m^2)}(u + mw) \quad (19)$$

$$w'' + 2(y + a_o) w' = \frac{M}{(1+m^2)}(mu - w) \quad (20)$$

$$\theta'' + 2(\text{Pr})(y + a_o) \theta' - (R)(\text{Pr})(\theta - 1) = 0 \quad (21)$$

Where  $a_o = \frac{\nu_o}{2}$ . All the symbols are defined in nomenclature. Of special significance for this type of flow and heat and mass transfer situation are the skin-friction coefficient and the Nusselt number  $Nu$ . The skin-friction coefficients in the  $x'$ - direction and  $z'$ - direction, the local Nusselt number and the local Sherwood number are, respectively given by

$$\left. \begin{aligned} \tau_x = \mu \frac{\partial u'}{\partial y'} \Big|_{y'=0} = \frac{\mu u_o}{h} u'(0) \Rightarrow \tau_1 = \frac{2\tau_x}{\rho u_o^2} = 2 \text{Re}^{-1} u'(0) \text{ and} \\ \tau_z = \mu \frac{\partial w'}{\partial y'} \Big|_{y'=0} = \frac{\mu u_o}{h} w'(0) \Rightarrow \tau_2 = \frac{2\tau_z}{\rho u_o^2} = 2 \text{Re}^{-1} w'(0) \end{aligned} \right\} \quad (22)$$

$$q_w = -k \frac{\partial T'}{\partial y'} \Big|_{y'=0} = [-\theta'(0)](T'_w - T'_\infty) \frac{k}{h} \Rightarrow Nu = \frac{q_w}{(T'_w - T'_\infty) k} = -\theta'(0) \quad (23)$$

Where  $Re = \frac{u_o h}{\nu}$  is the Reynold's number.

### 3. Numerical Solutions By Finite Element Method

**3.1. Finite Element Method** The finite element method (FEM) is a numerical and computer based technique of solving a variety of practical engineering problems that arise in different fields such as, in heat transfer, fluid mechanics (Bhargava and Rana [21]), chemical processing (Lin and Lo [22]), rigid body dynamics (Dettmer and Peric [23]), solid mechanics (Hansbo and Hansbo [24]) and many other fields. It is recognized by developers and users as one of the most powerful numerical analysis tools ever devised to analyze complex problems of engineering. The sophistication of the method, its accuracy, simplicity, and computability all make it a widely used tool in the engineering modelling and design process. It has been applied to a number of physical problems, where the governing differential equations are solved by transforming them into a matrix equation. The primary feature of FEM is its ability to describe the geometry or the media of the problem being analyzed with great flexibility. This is because the discretization of the domain of the problem is performed using highly flexible uniform or non uniform patches or elements that can easily describe complex shapes. The method essentially consists in assuming the piecewise continuous function for the solution and obtaining the parameters of the functions in a manner that reduces the error in the solution. An excellent description of finite element formulations is available in Bathe [25] and Reddy [26]. The steps involved in the finite element analysis areas follows.

**3. 1. 1. Discretization of the Domain:** The basic concept of the FEM is to divide the domain or region of the problem into small connected patches, called finite elements. The collection of elements is called the finite element mesh. These finite elements are connected in a non overlapping manner, such that they completely cover the entire space of the problem.

#### 3. 1. 2. Generation of the Element Equations:

- A typical element is isolated from the mesh and the variational formulation of the given problem is constructed over the typical element.
- Over an element, an approximate solution of the variational problem is supposed, and by substituting this in the system, the element equations are generated.
- The element matrix, which is also known as stiffness matrix, is constructed by using the element interpolation functions.

These steps results in a matrix equation of the form  $[K^e]\{u^e\} = \{F^e\}$ , which defines the finite element model of the original equation.

**3. 1. 3. Assembly of the Element Equations:** The algebraic equations so obtained are assembled by imposing the inter element continuity conditions. This yields a large number of algebraic equations known as the global finite element model, which governs the whole domain.

**3. 1. 4. Imposition of the Boundary Conditions:** On the assembled equations, the Dirichlet's and Neumann boundary conditions (17) are imposed.

**3. 1. 5. Solution of Assembled Equations:** The assembled equations so obtained can be solved by any of the numerical techniques, namely, Gauss elimination method, LU decomposition method, and

the final matrix equation can be solved by a direct or indirect (iterative) method. For computational purposes, the coordinate  $y$  is varied from 0 to  $y_{\max} = 10$ , where  $y_{\max}$  represents infinity *i.e.*, external to the momentum, energy and concentration boundary layers. The whole domain is divided into a set of 40 line segments of equal width 0.1, each element being two-noded.

In one-dimensional space, linear element, quadratic element, or element of higher order can be taken. The whole domain is divided into a set of 40 intervals of equal length 0.1. At each node three functions are to be evaluated. Hence after assembly of the elements we obtain a set of 123 equations which are nonlinear. Therefore, an iterative scheme must be utilized in the solution. After imposing the boundary conditions, a system of equations has been obtained which is solved by the Gauss elimination method while maintaining an accuracy of 0.00005. A convergence criterion based on the relative difference between the current and previous iterations is employed. When these differences satisfy the desired accuracy, the solution is assumed to have been converged and iterative process is terminated. The Gaussian quadrature is implemented for solving the integrations. The code of the algorithm has been executed in MATLAB “bvp4c” running on a PC. Excellent convergence was achieved for all the results.

#### 4. Study of Grid Independence of Finite Element Method

Table 1. Grid Invariance test for primary velocity, secondary velocity and temperature profiles at  $\gamma = 0.5$

Mesh (Grid) Size = 0.0001			Mesh (Grid) Size = 0.001		
$u$	$w$	$\theta$	$u$	$w$	$\theta$
0.0000000000	0.0000000000	1.0000000000	0.0000000000	0.0000000000	1.0000000000
0.7234765887	0.2388297170	0.9743975401	0.7232695222	0.2387289256	0.9740068913
0.8706516027	0.3663154840	0.9391090870	0.8701688051	0.3660761118	0.9382099509
0.8546831608	0.4013786912	0.8931466937	0.8538790941	0.4009748697	0.8916516900
0.7927082181	0.3905737996	0.8354807496	0.7915706635	0.3899961710	0.8333606124
0.7131123543	0.3587989509	0.7647858262	0.7116740942	0.3580629230	0.7620986700
0.6202089190	0.3155803680	0.6786968708	0.6185632348	0.3147315979	0.6756160259
0.5118013620	0.2630710304	0.5725184679	0.5101124048	0.2621920109	0.5693576336
0.3824672103	0.1994354427	0.4371592700	0.3809781671	0.1986510009	0.4343856573
0.2214809209	0.1180272698	0.2559509277	0.2205180824	0.1175117642	0.2541863024
0.0000000000	0.0000000000	0.0000000000	0.0000000000	0.0000000000	0.0000000000

To investigate the sensitivity of the solutions to mesh density, it was observed that in the same domain the accuracy is not affected, even if the number of elements is increased, by decreasing the size of the elements. This serves only to increase the compilation times and does not enhance in any way the accuracy of the solutions, as shown in table 1. Thus, for computational purposes, 1000 elements were taken for presentation of the results. Excellent convergence was achieved in the present study.

**5. Program Code Validation:**

In order to ascertain the accuracy of the numerical results, the present results are compared with the previous analytical results of Mohamed Seddeek and Emad Aboeldahab [17] in table 2 when  $\gamma = 0$ . They are found to be in an excellent agreement. Also, concluded a set of results corresponding to various special cases.

- (i) Substitute  $M = 0, m = 0, R = 0$  and  $\gamma = 0$  in equations (19), (20) and (21) yields identical results to those well known in hydrodynamics (Schlichting [21]).
- ii) Substitute  $m = 0, R = 0$  and  $\gamma = 0$  in equations (19), (20) and (21) yields identical results to those well known in (Nirmal et al. [27]).

Table 2:  $(\tau_1 \ \& \ \tau_2)$  is the Skin-friction results obtained in the present study and  $(\tau_1^* \ \& \ \tau_2^*)$  is the Skin-friction results obtained by Mohamed Seddeek and Emad Aboeldahab [17] when  $\gamma = 0$

$m$	$R$	$M$	$\tau_1$	$\tau_1^*$	$\tau_2$	$\tau_2^*$
0.5	0.1	5.0	6.822532	6.82251	- 1.960668	- 1.960666
0.7	0.1	5.0	7.951355	7.95135	- 2.926234	- 2.92623
0.5	0.1	7.0	3.179777	3.17976	- 3.655797	- 3.65579
0.5	0.4	5.0	7.358323	7.35839	- 1.945116	- 1.945116

**6. Results and Discussions:**

We solve the similarity equations (19), (20) and (21) numerically subject to the boundary conditions given by (17). Graphical representations of the numerical results are illustrated in figure (2) through figure (13) to show the influences of different parameters on the boundary layer flow. During the course of numerical calculations of the primary velocity, secondary velocity and temperature, the values of the Prandtl number are chosen for Mercury ( $Pr = 0.025$ ), Air at  $25^\circ C$  and one atmospheric pressure ( $Pr = 0.71$ ), Water ( $Pr = 7.00$ ) and Water at  $4^\circ C$  ( $Pr = 11.40$ ). To examine the effect of parameters related to the problem on the velocity field and skin-friction numerical computations are carried out at  $Pr = 0.71$ . To find solution of this problem, we have placed an infinite vertical plate in a finite length in the flow. Hence, we solve the entire problem in a finite boundary. However, in the graphs, the  $y$  values vary from 0 to 10, and the velocity, temperature, and concentration tend to zero as  $y$  tend to 10. This is true for any value of  $y$ . Thus, we have considered finite length.

**6. 1. Effect of Grashof number for heat transfer,  $Gr$ .** Figs. 1 and 2 show that the primary velocity and the secondary velocity increase with an increase in Grashof number  $Gr$ . Grashof number  $Gr$  signifies the relative effect of the thermal buoyancy force to the viscous hydrodynamic force. As expected, it is observed that there is a rise in the fluid velocity due to the enhancement of thermal buoyancy force. It is due to the fact that an increase of Grashof number has a tendency to increase the thermal effect.

**6. 2. Effect of Magnetic field parameter,  $M$ .** Figs. 3 and 4 display the effect of magnetic parameter ( $M$ ) on primary and secondary velocities. It is seen from these figures that the primary as well as secondary velocity falls when  $M$  increases. That is the primary or secondary fluid motion is retarded due to application of transverse magnetic field. This phenomenon clearly agrees to the fact that Lorentz force that appears due to interaction of the magnetic field and fluid velocity resists the fluid motion.

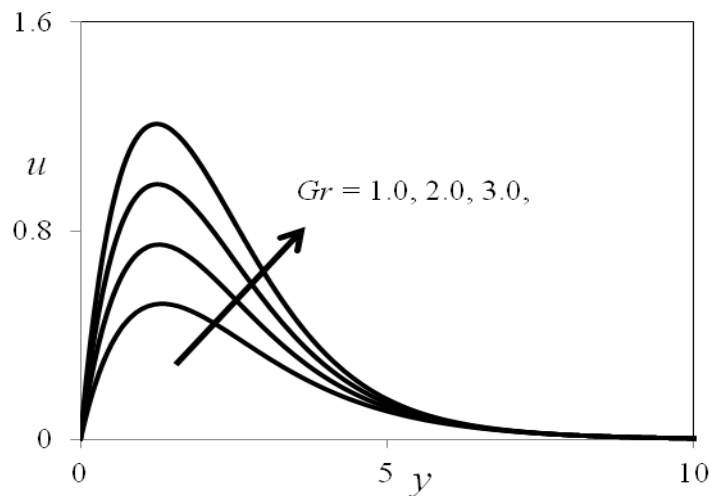


Fig. 1. Effect of  $Gr$  on primary velocity profiles

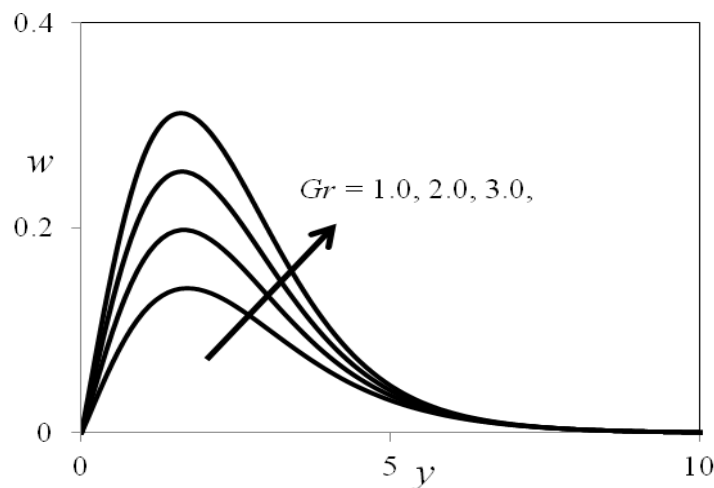


Fig. 2. Effect of  $Gr$  on secondary velocity profiles

**6. 3. Effect of Hall parameter,  $m$ .** Figure (5) depicts the primary velocity profiles as the Hall parameter increases. We see that  $u$  increases as increases. It can also be observed that velocity profiles approach their classical values when the Hall parameter becomes large ( $m > 5$ ). In figure (6), we see that  $w$  profiles increase for  $m < 1$  and decrease for  $m > 1$ .

**6. 4. Effect of thermal radiation parameter,  $R$ .** The effects of the thermal radiation parameter on the primary velocity and temperature profiles in the boundary layer are illustrated in figures (7) and (8) respectively. Increasing the thermal radiation parameter produces significant increase in the thermal condition of the fluid and its thermal boundary layer. This increase in the fluid temperature induces more flow in the boundary layer causing the velocity of the fluid there to increase. The effect of thermal radiation parameter on secondary velocity profiles is shown in the figure (9). From this figure, we observe that the secondary velocity is increasing with increasing values of thermal radiation parameter.

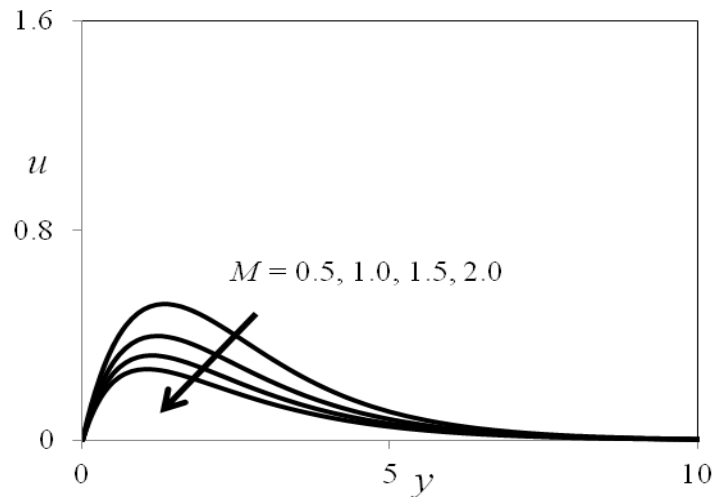


Fig. 3. Effect of  $M$  on primary velocity profiles

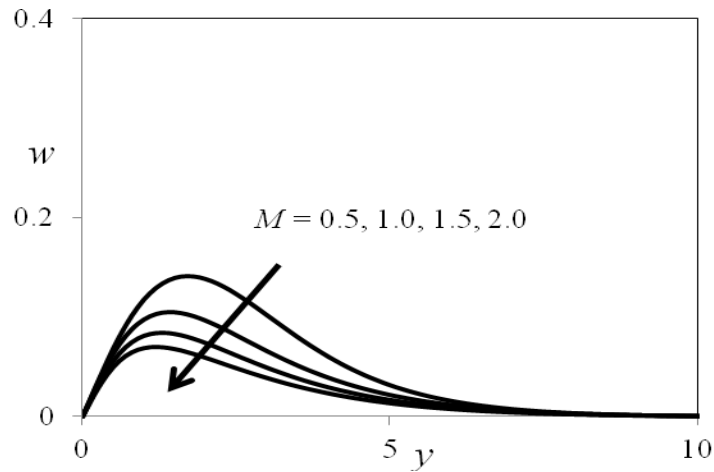


Fig. 4. Effect of  $M$  on secondary velocity profiles

**6. 5. Effect of Prandtl number,  $Pr$ .** The Prandtl number is the ratio of momentum diffusivity to the thermal diffusivity. Figure (10) illustrates the temperature profiles for different values of Prandtl number. From this figure, it is observed that an increase in the Prandtl number results a decrease of the thermal boundary layer thickness and in general lower average temperature within the boundary layer. The reason is that smaller values of Prandtl number are equivalent to increasing the thermal conductivities, and therefore heat is able to diffuse away from the heated surface more rapidly than for higher values of  $Pr$ . This is because, either increase of kinematic viscosity or decrease of thermal conductivity leads to increase in the value of Prandtl number. Hence temperature decreases with increasing of Prandtl number.

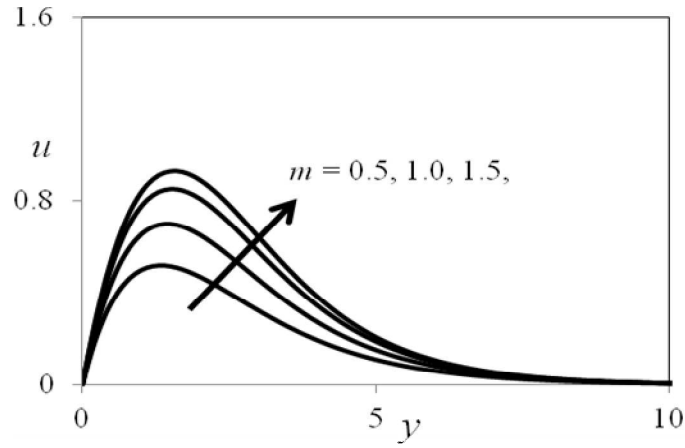


Fig. 5. Effect of  $m$  on primary velocity profiles

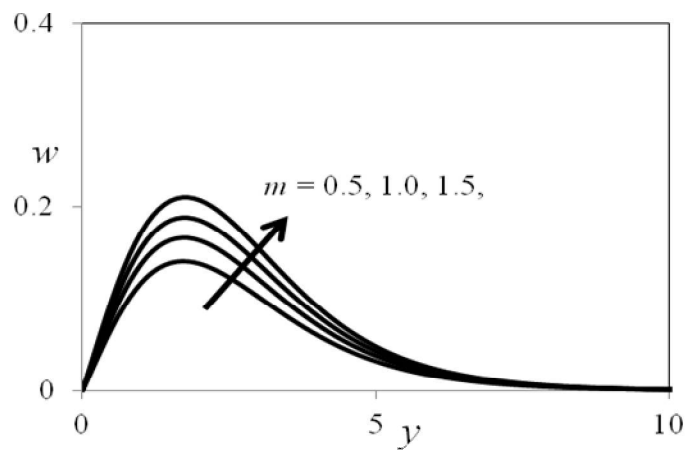


Fig. 6. Effect of  $m$  on secondary velocity profiles

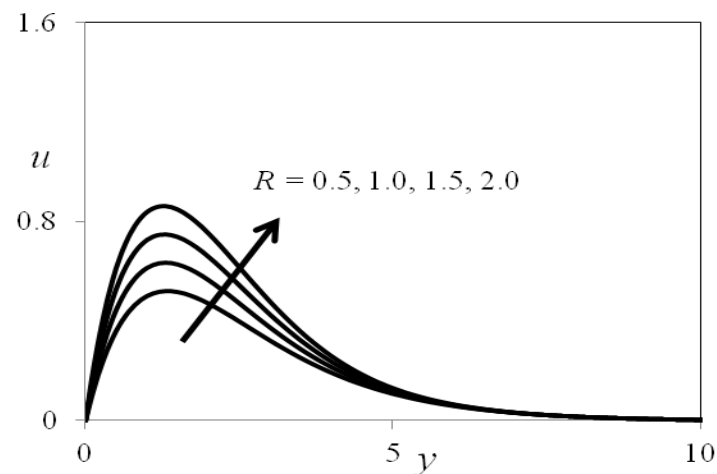


Fig. 7. Effect of  $R$  on primary velocity profiles

**6. 6. Influence Of Casson Fluid Parameter,  $\gamma$ .** The velocity profile in the Fig. 11 shows that rate of motion is significantly reduced with increasing of Casson fluid parameter. Also, it is observed from this Fig. 11, the boundary layer momentum thickness decreases as increase of Casson fluid parameter.

**6. 7. Skin-friction and Nusselt number:** The skin-friction values due to primary and secondary velocities are evaluated from Eq. (22) as a function of the axial coordinate is shown in table 3. The local wall shear stress increases with increasing thermal radiation parameter. The value of the skin-friction becomes negative, which implies that after some time there occurs a reverse type of flow near the moving plate. Physically this is also true as the motion of the fluid is due to plate moving in the vertical direction against the gravitational field. The observation from table 3, the skin-friction increases with the increase of Hall parameter and the rate of heat transfer increases with increasing values of the radiation parameter. The Local Nusselt number for different values of the radiation parameter and Prandtl number are shown in table 4. The trend shows that the Local Nusselt number increases with increasing radiation parameter and decreases with rising values of Prandtl number.

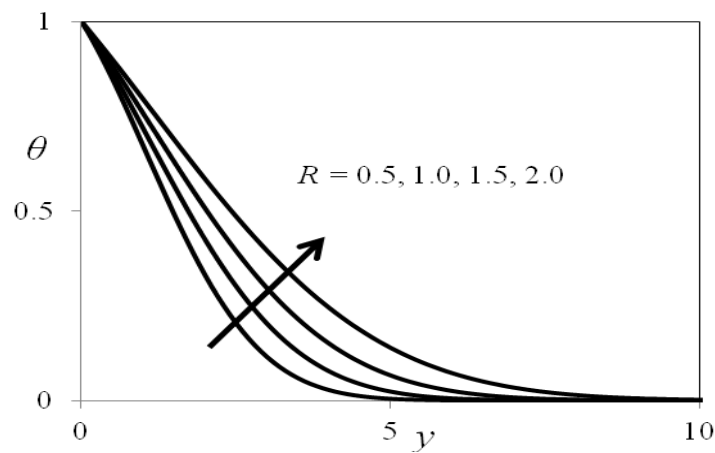


Fig. 8. Effect of  $R$  on temperature profiles

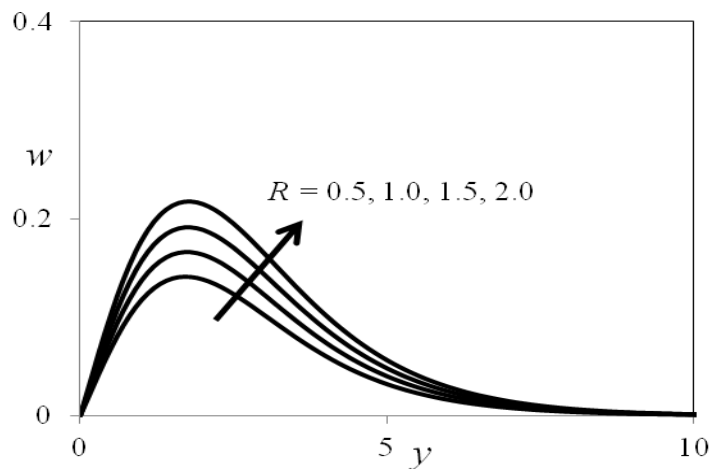


Fig. 9. Effect of  $R$  on secondary velocity profiles

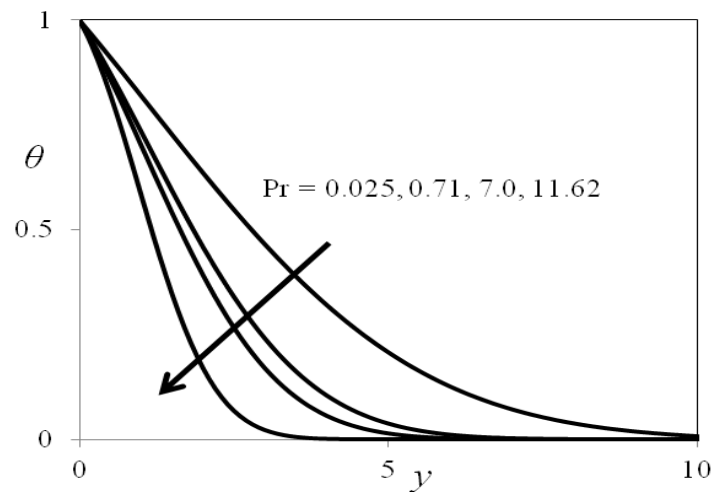


Fig. 10. Effect of Pr on temperature profiles

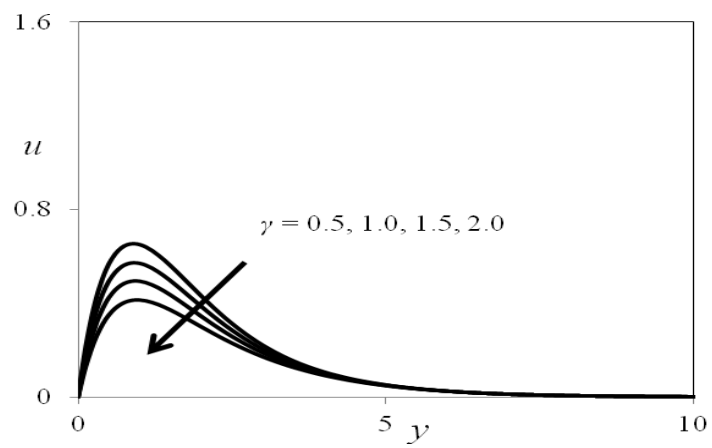


Fig. 11. Effect of  $\gamma$  on temperature profiles

Table 3: Skin-friction ( $\tau_1$  &  $\tau_2$ ) results

$M$	$m$	$R$	$\tau_1$	$\tau_2$
5.0	0.5	0.1	6.84817254	-1.90448721
7.0	0.5	0.1	3.25402586	-3.54925469
5.0	0.7	0.1	7.94225137	-2.88492594
5.0	0.5	0.4	7.372948051	-1.90549712

Table 4. Rate of heat and mass transfer values

Pr	R	Nu
0.71	0.1	5.93614498
7.00	0.1	4.01797759
0.71	0.4	6.15974892

## 7. Conclusions:

This work investigated the combined effects of hall current and thermal radiation on an unsteady MHD free convective Casson fluid flow near a vertical plate in presence of heat transfer. The similarity solutions were obtained using suitable transformations and the resulting similarity ordinary differential equations were solved by using finite element method. A parametric study illustrating the influence of different flow parameters on primary velocity, secondary velocity and temperature are investigated. (i). The Grashof number has an accelerating effect on the flow velocity due to the enhancement in the buoyancy force. (ii). Thermal buoyancy force tends to retard the secondary fluid velocity throughout the boundary layer region. (iii). Hall parameter tends to accelerate both the primary and secondary fluid velocities throughout the boundary layer region. (iv). Finally, the analytical solutions and the numerical solutions were compared and the numerical comparisons showed an excellent compatible between the values.

## References

- [1] Baltacıoğlu, A.K., Civalek, O., Akgöz, B., Demir, F., Large deflection analysis of laminated composite plates resting on nonlinear elastic foundations by the method of discrete singular convolution. *International Journal of Pressure Vessels and Piping*, 88, 290-300, 2011.
- [2] Shu, C., Chew, Y.T., Richards, B.E., Generalized differential and integral quadrature and their application to solve boundary layer equations. *International Journal for Numerical Methods in Fluids*, 1995.
- [3] Civalek, O., Korkmaz, A., Demir, C., Discrete singular convolution approach for buckling analysis of rectangular Kirchhoff plates subjected to compressive loads on two-opposite edges. *Advances in Engineering Software*, 41, 557-560, 2010.
- [4] Ramana Murthy, M.V., Srinivasa Raju, R., Anand Rao, J., Heat and mass transfer effects on MHD natural convective flow past an infinite vertical porous plate with thermal radiation and Hall current. *Procedia Engineering Journal*, 127, 1330-1337, 2015.
- [5] Rao, V.S., Babu, L.A., Raju, R.S., Finite element analysis of radiation and mass transfer flow past semi-infinite moving vertical plate with viscous dissipation. *Journal of Applied Fluid Mechanics*, 6, 321-329, 2013.
- [6] Srinivasa Raju, R., Combined influence of thermal diffusion and diffusion thermo on unsteady hydromagnetic free convective fluid flow past an infinite vertical porous plate in presence of chemical reaction. *Journal of Institution of Engineers: Series C*, 97(4), 505-515, 2016.
- [7] Srinivasa Raju, R., Effects Of Soret And Dufour On Natural Convective Fluid Flow Past A Vertical Plate Embedded In Porous Medium In Presence Of Thermal Radiation Via FEM, *Journal of the Korean Society for Industrial and Applied Mathematics*, 20(4), 309-332, 2016.

- [8] Srinivasa Raju, R., Anitha, G., Jitthender Reddy, G., Influence of Transpiration and Hall effects on unsteady MHD free convection fluid flow over an infinite vertical plate. *International Journal of Control Theory and Applications*, 9(23), 455-462, 2016.
- [9] Srinivasa Raju, R., Anil Kumar, M., Dharmendar Reddy, Y., Unsteady MHD Free Convective Flow Past A Vertical Porous Plate With Variable Suction. *ARPN Journal of Engineering and Applied Sciences*, 11(23), 13608-13616, 2016.
- [10] Sailaja, S.V., Shanker, B., Srinivasa Raju, R., Double Diffusive Effects On MHD Mixed Convection Casson Fluid Flow Towards A Vertically Inclined Plate Filled In Porous Medium In Presence Of Biot Number: A Finite Element Technique, *Journal of Nanofluids*, 2016 (In press).
- [11] Sarpkaya, T., Flow of non-Newtonian fluids in a magnetic field. *American Institute of Chemical Engineering*, 7, 324-328, 1961.
- [12] Mukhopadhyay, S., De, P.R., Bhattacharyya, K., Layek, G.C., Casson fluid flow over an unsteady stretching surface. *Ain Shams Engineering Journal*, 4, 933-938, 2013.
- [13] Mukhopadhyaya, S., Moindala, I.C., Hayat, T., MHD boundary layer flow of Casson fluid passing through an exponentially stretching permeable surface with thermal radiation. *Chinese Physics Letters*, 23, 104701, 2014.
- [14] Raju, C.S.K., Sandeep, N., Sugunamma, V., Babu, M.J., Reddy, J.V.R., Heat and mass transfer in magnetohydrodynamic Casson fluid over an exponentially permeable stretching surface. *Engineering Science and Technology, International Journal*, 19(1), 45-52, 2016.
- [15] Das, M., Mahato, R., Nandkeolyar, R., Newtonian heating effect on unsteady hydro-magnetic Casson fluid flow past a flat plate with heat and mass transfer. *Alexandria Engineering Journal*, 2015, <http://dx.doi/10.1016/j.aej.2015.07.007>.
- [16] Mahanta, G., Shaw, S., 3D Casson fluid flow past a porous linearly stretching sheet with convective boundary condition. *Alexandria Engineering Journal*, 2015.
- [17] Seddeek, Md., Emad Aboeldahab, M., Radiation effects on unsteady MHD free convection with hall current near an infinite vertical porous plate. *International Journal of Applied Mathematics and Mechanics*, 26(4), 249-255, 2001.
- [18] Dash, R. K., Mehta, K. N., Jayaraman, G., Casson Fluid Flow in a Pipe Filled with a Homogeneous Porous Medium. *International Journal of Engineering Science*, 34, 1145-1156, 1996.
- [19] Cogley, A. C., Vincenty, W. E., Gilles, S. E., Differential approximation for radiation in a non-gray gas near equilibrium, *AIAA Journal*, 6, 551-553, 1968.
- [20] Schlichting, H., *Boundary Layer Theory*. McGraw-Hill New York, 1968.
- [21] Bhargava, R., Rana, P., Finite element solution to mixed convection in MHD flow of micropolar fluid along a moving vertical cylinder with variable conductivity. *International Journal of Applied Mathematics and Mechanics*, 7, 29-51, 2011.
- [22] Lin, Y. Y., Lo, S. P., Finite element modeling for chemical mechanical polishing process under different back pressures. *J. Mat. Proc. Tech.*, 140(1-3), 646-652, 2003.
- [23] Dettmer, W., Peric, D., A computational framework for fluid-rigid body interaction, finite element formulation and applications, *Computer Methods in Applied Mechanics in Engineering*, 195(13-16), 1633-1666, 2006.
- [24] Hansbo, A., Hansbo, P., A finite element method for the simulation of strong and weak discontinuities in solid mechanics, *Computer Methods in Applied Mechanics in Engineering*, 193(33-35), 3523-3540, 2004.
- [25] Bathe, K. J., *Finite Element Procedures*. Prentice-Hall New Jersey, 1996.
- [26] Reddy, J. N., *An Introduction to the Finite Element Method*. McGraw-Hill New York, 1985.
- [27] Nirmal, C. S., Rallath, H., Singh, A. K., An exact solution for unsteady MHD free convection flow with constant heat flux. *International Journal Communications in Heat Mass Transfer*, 21, 131-315, 1994.